

$$Y \sim \beta_0 + \beta$$

## WEEK 2: THE GENERAL LINEAR MODEL

Boris Bernhardt, PhD

Bratislav Misic, PhD



## WELCOME + GENERAL ORGANIZATION

EVERY FRIDAY 10.30-13.30

NEURO – BT100

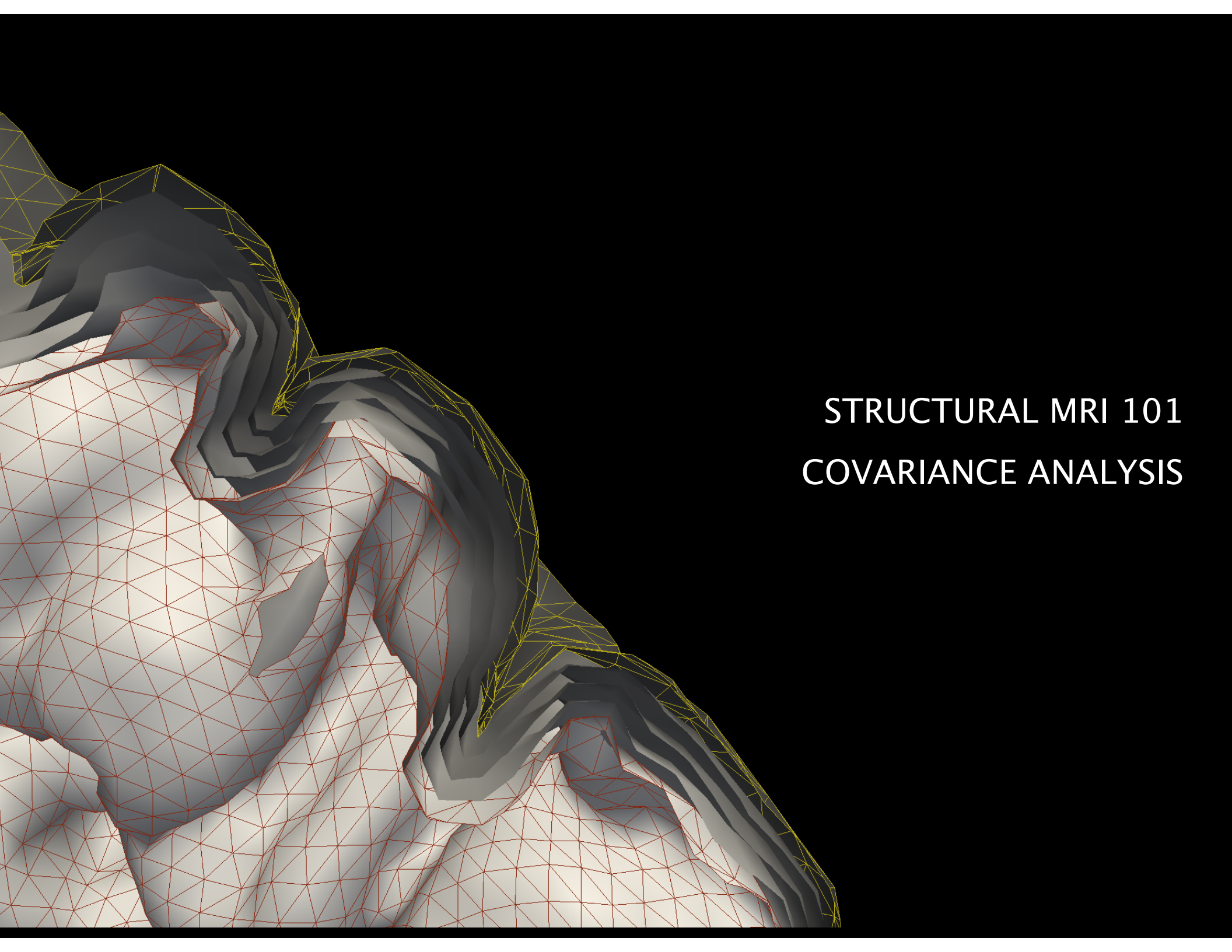
[boris.bernhardt@mcgill.ca](mailto:boris.bernhardt@mcgill.ca)

[bratislav.misic@mcgill.ca](mailto:bratislav.misic@mcgill.ca)

## MOCK PAPER

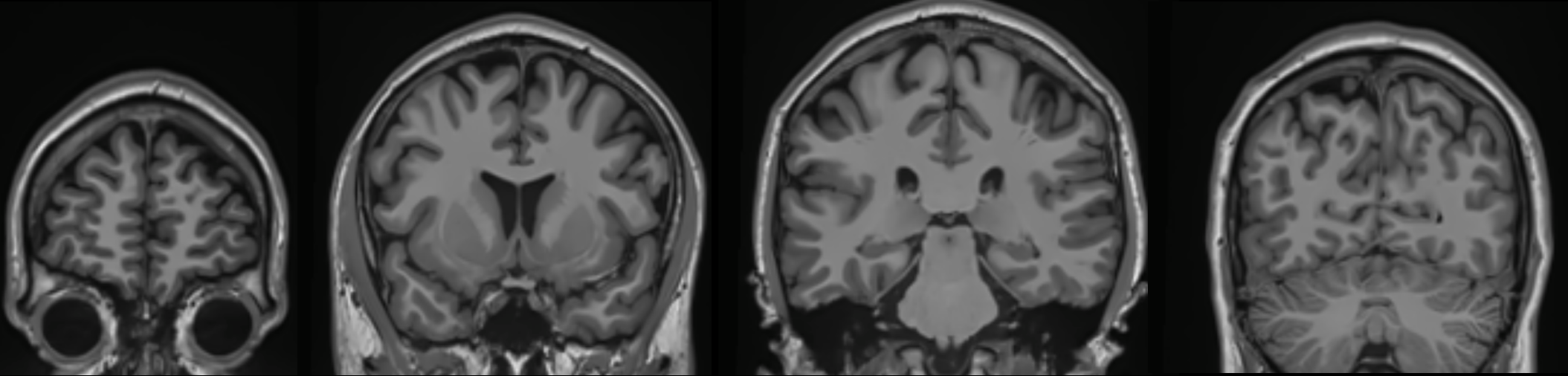
We will send you guidelines after the class:

- 1) Start thinking about it now
- 2) Discuss your ideas with your colleagues and with us
- 3) Prepare your proposal (about 10 pages)
- 4) Submit us your full version on Monday, October 29
- 5) We will give feedback by Friday, November 2
- 6) Deadline for final version is Monday, November 19
- 7) Presentation and discussion of the work on the last day of class  
(8 minutes PPT+ 4 min Q&A)



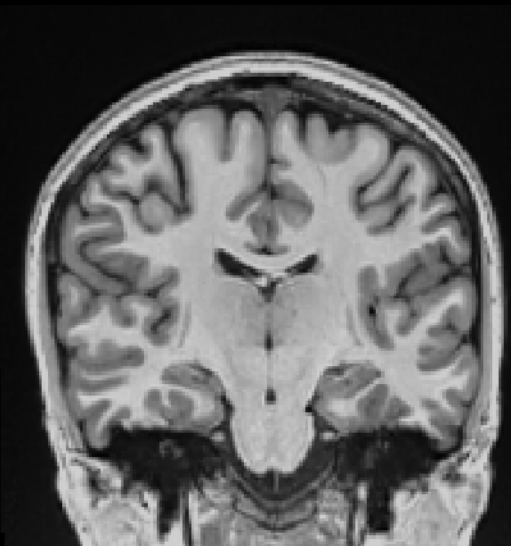
STRUCTURAL MRI 101  
COVARIANCE ANALYSIS

# structural MRI



T1-weighted MRI

# VOLUMETRY PIPELINE



input

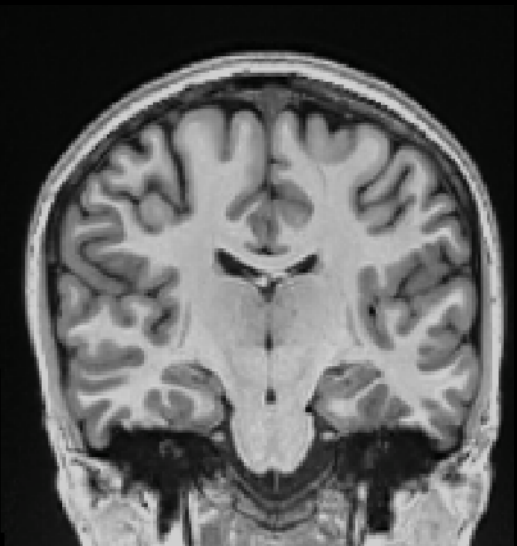


read and become expert

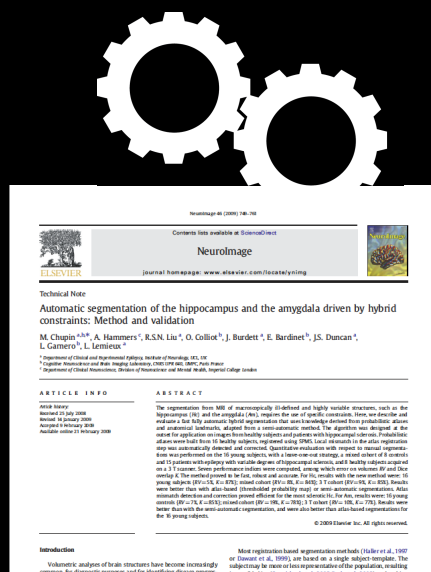


segment

# AUTOMATATION



input

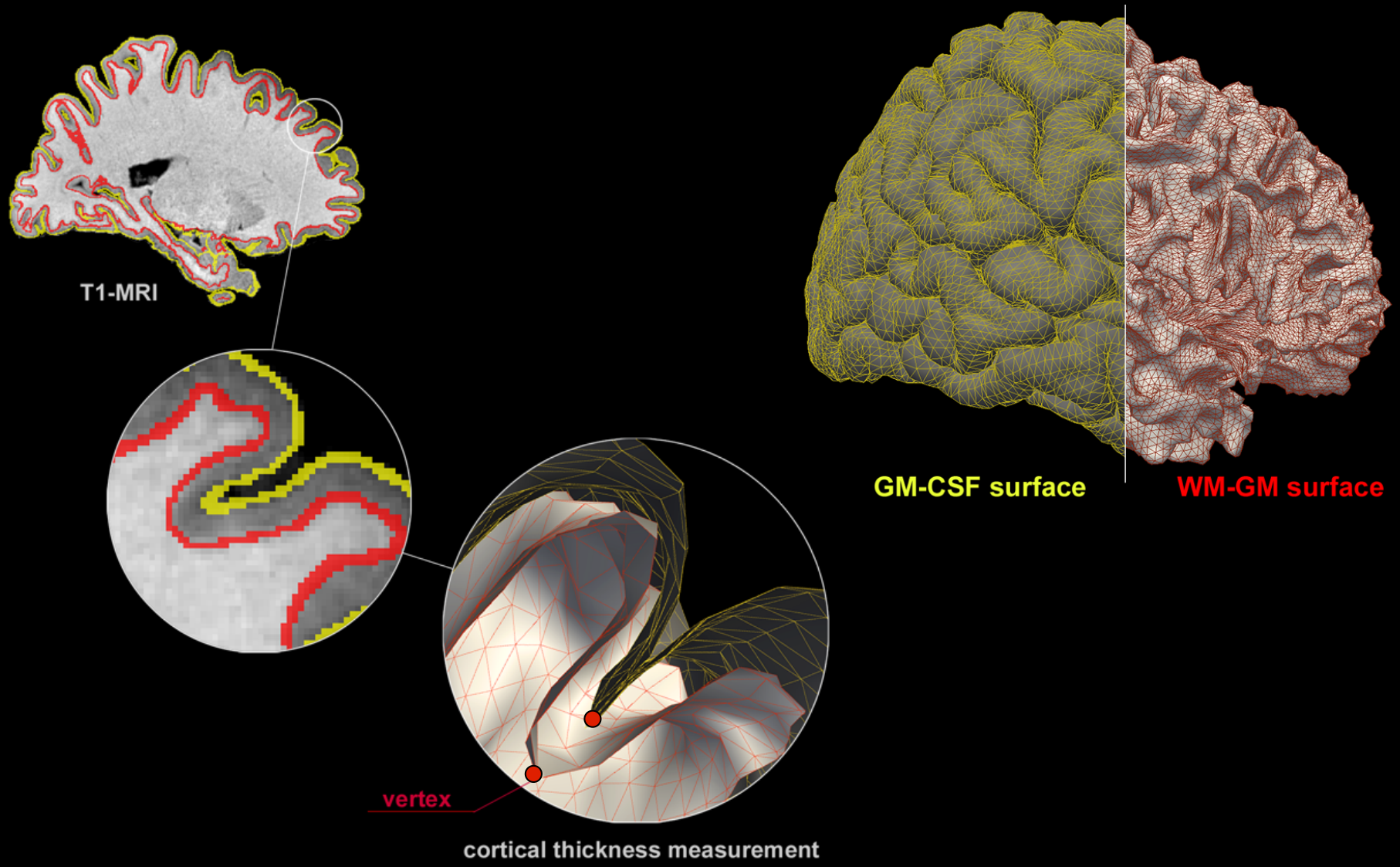


automatic segmentation approaches

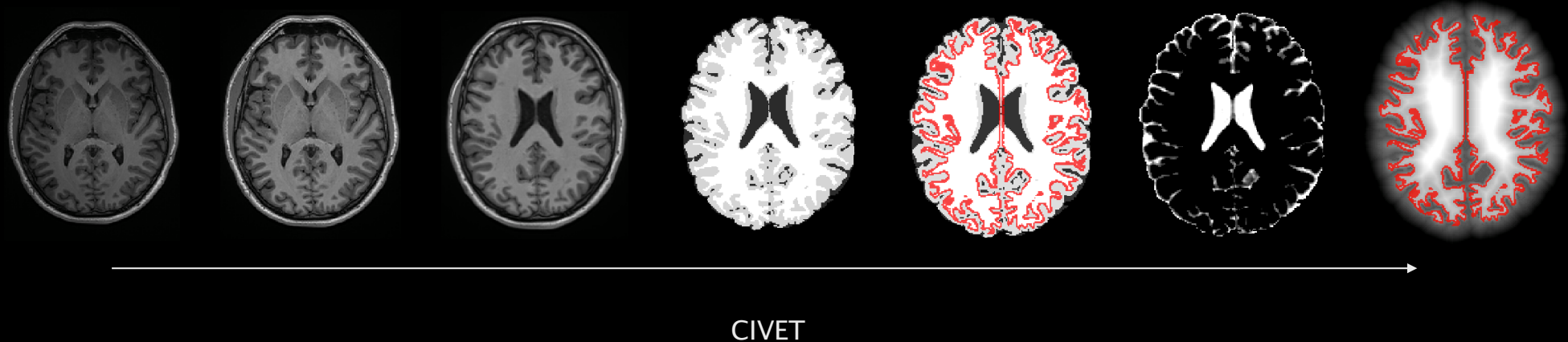


segment

# CORTICAL THICKNESS MEASUREMENT



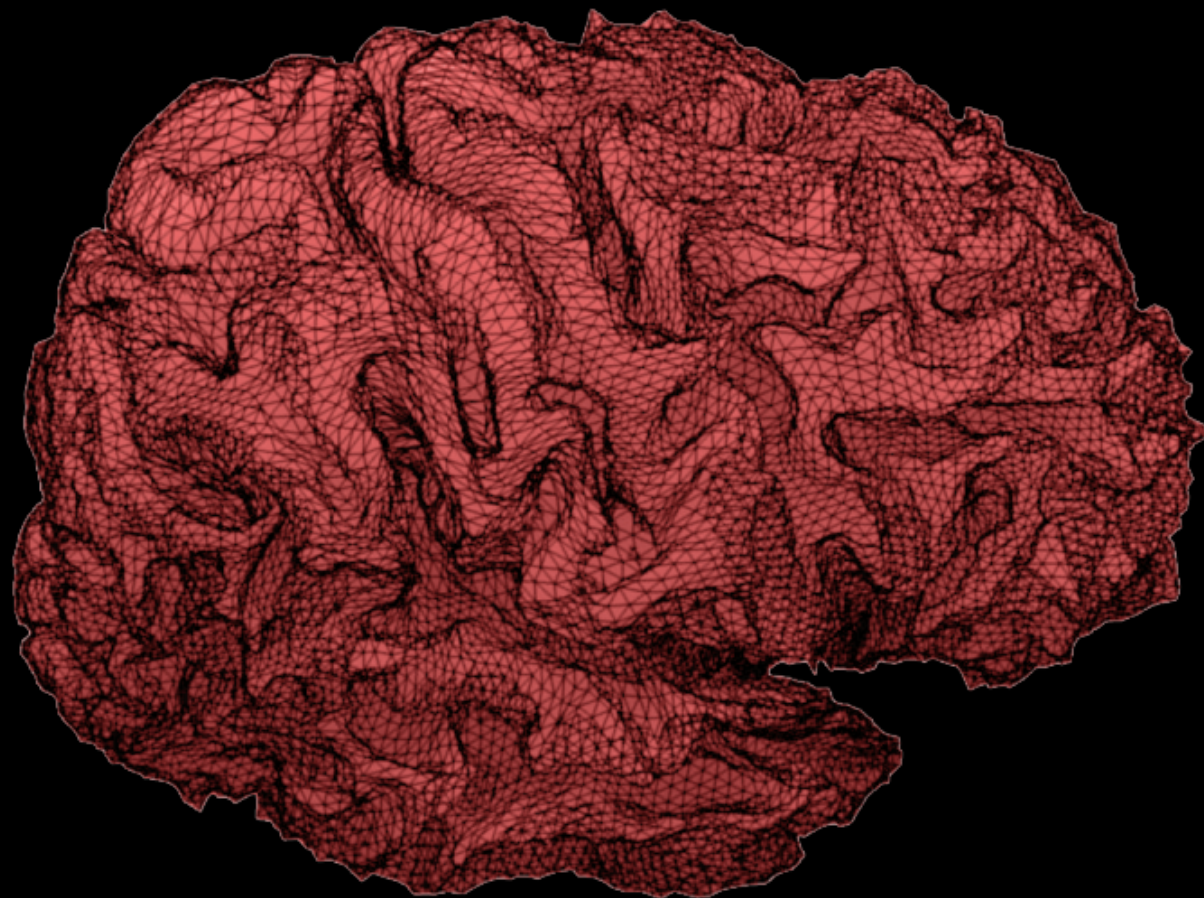
# PROCESSING PIPELINES



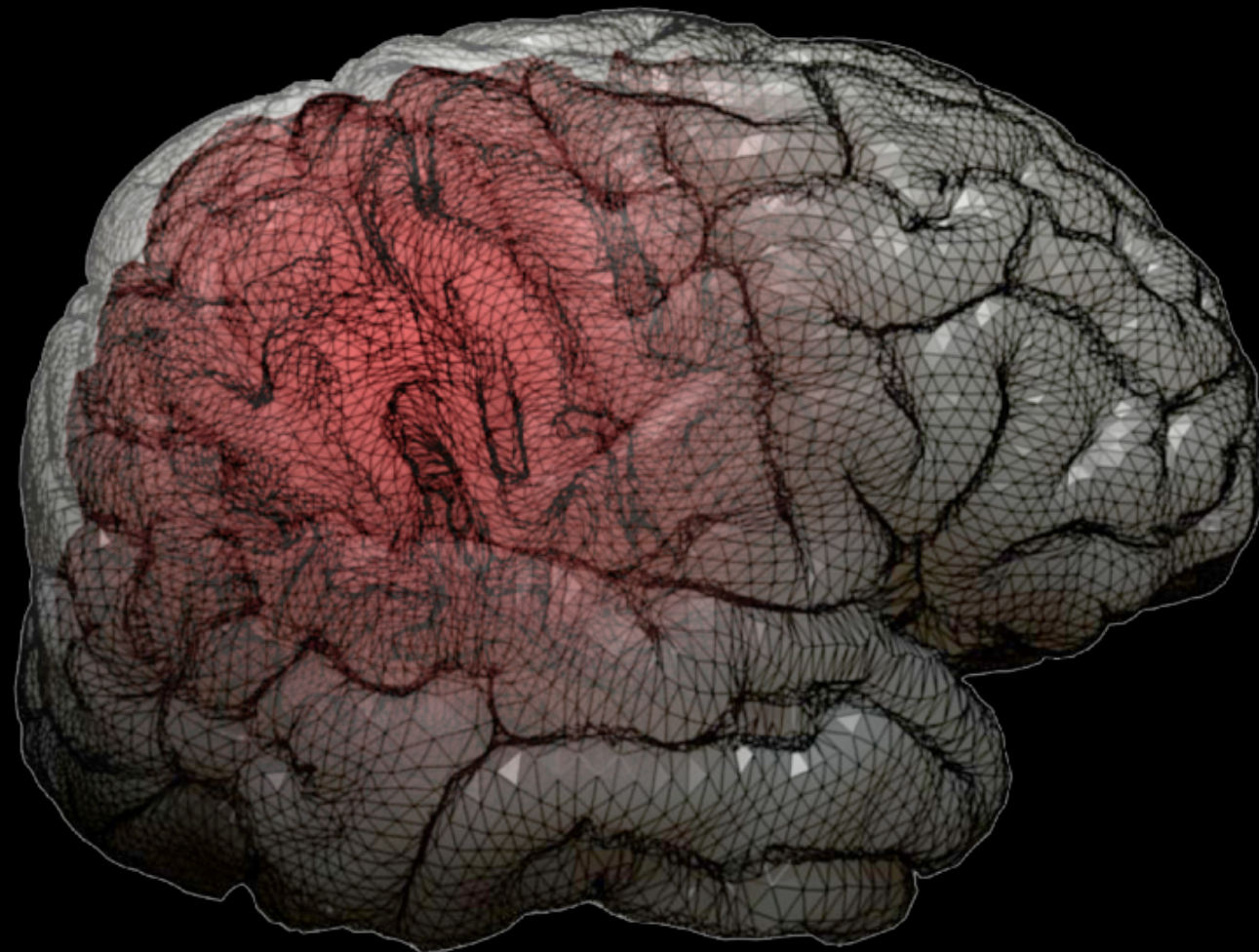
MacDonald et al. (2000) *NeuroImage*

Kim et al. (2005) *NeuroImage*

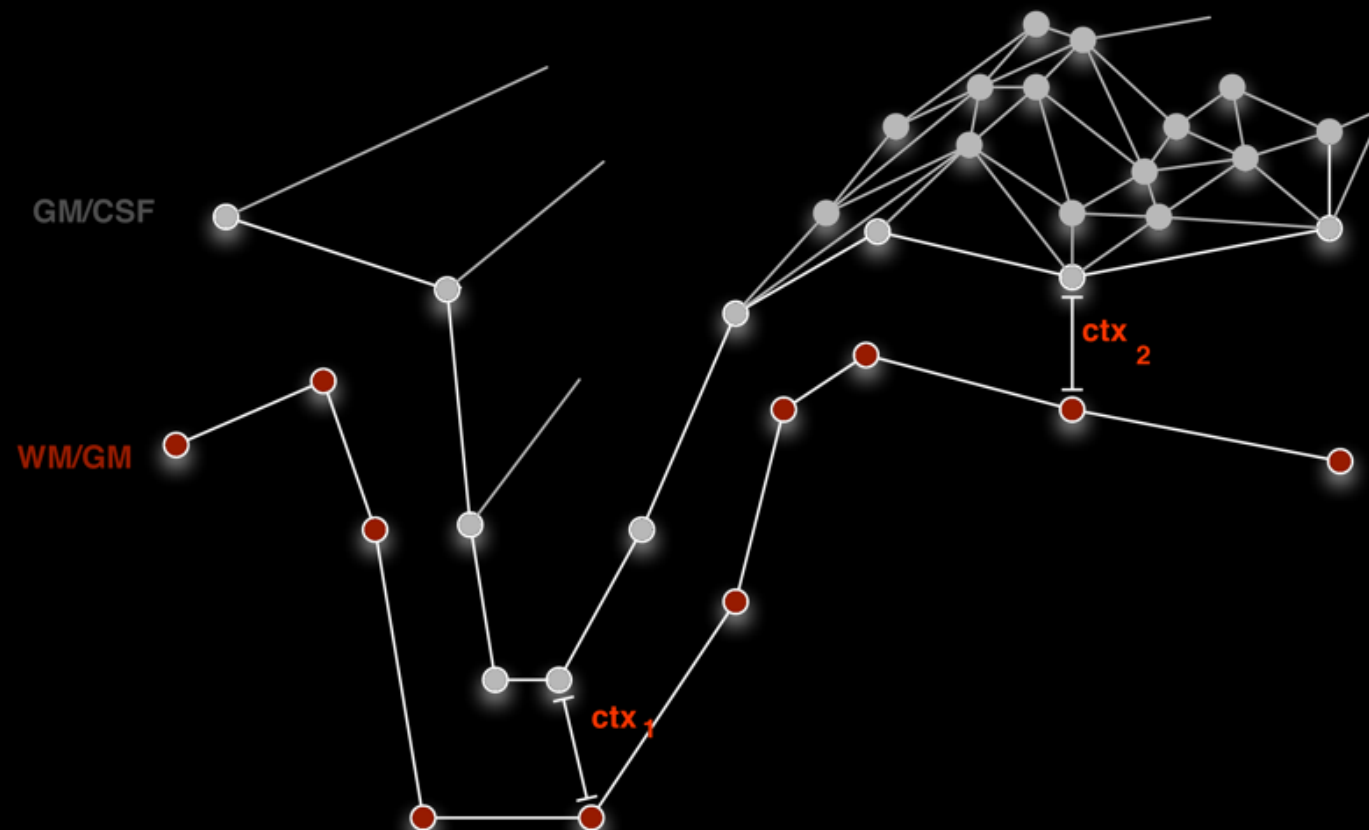
WM



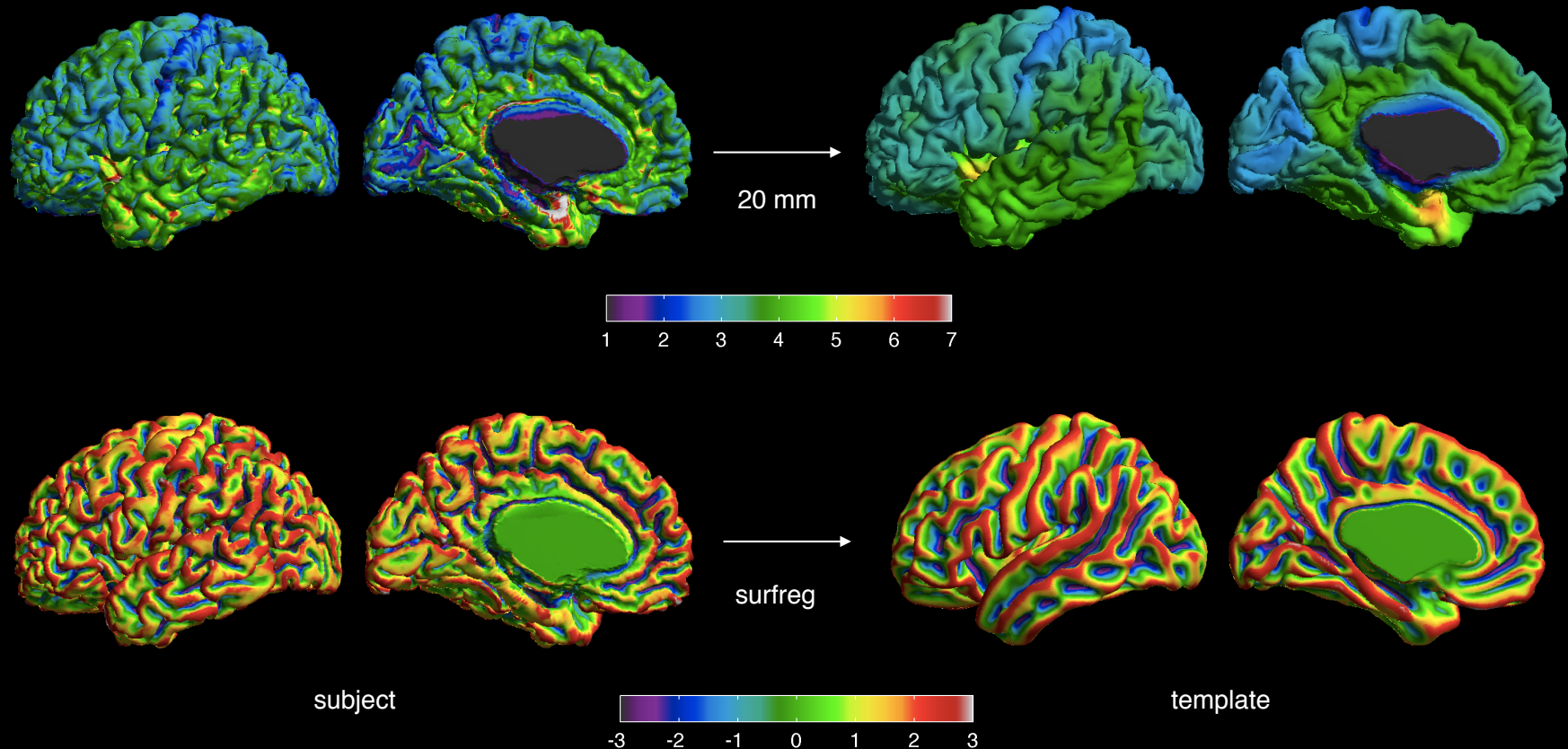
# GM SURFACE



# MEASUREMENT OF THICKNESS



# SURFACE-BASED PROCESSING



Chung et al. (2003) NeuroImage

Robbins et al. (2004) MedImaAnalysis

# NOW WE CAN FINALLY BUILD THE FIRST LINEAR MODELS

t-tests, correlations, partial correlations, ANOVAs, MANOVAs,...

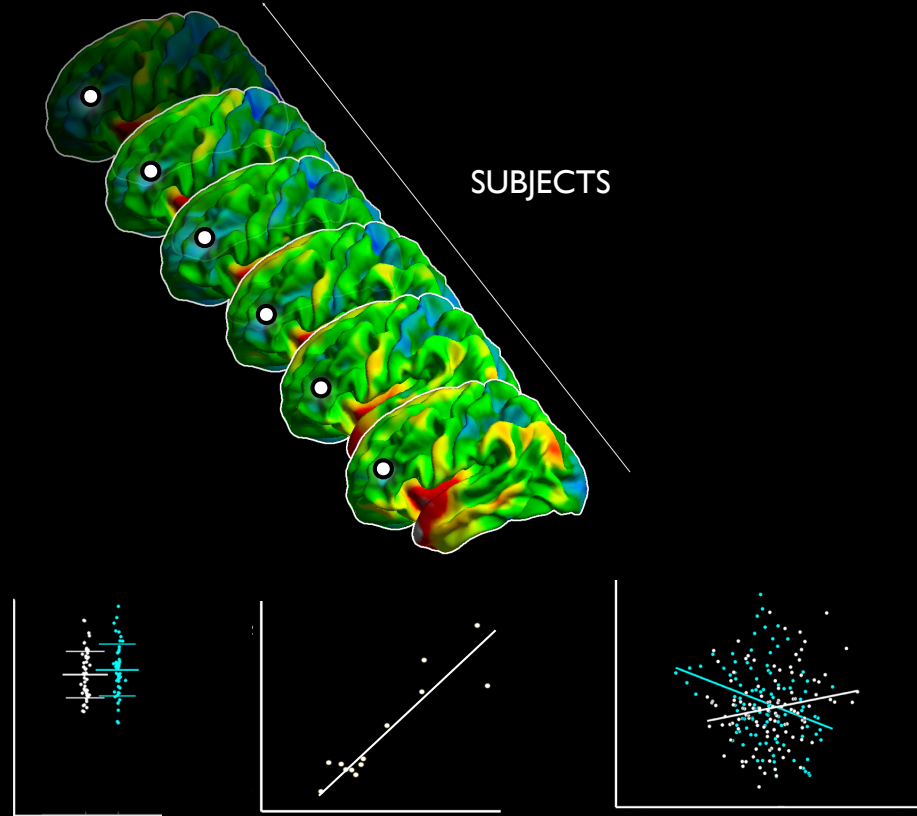
are just specific instances of the linear model of the form

$$Y \sim \beta_0 + \beta_1 * x_1 + \beta_2 * x_2 + \beta_3 * x_1 * x_2 + \dots + \varepsilon$$

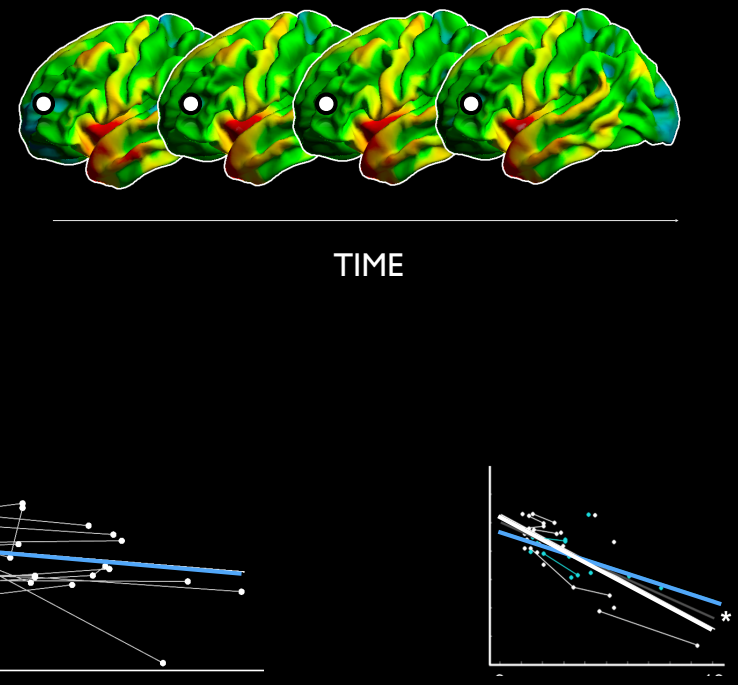
DATA                    INTERCEPT                    SIMPLE EFFECTS                    INTERACTIONS

## NOW WE CAN FINALLY BUILD THE FIRST LINEAR MODELS

CROSS-SECTIONAL ANALYSES

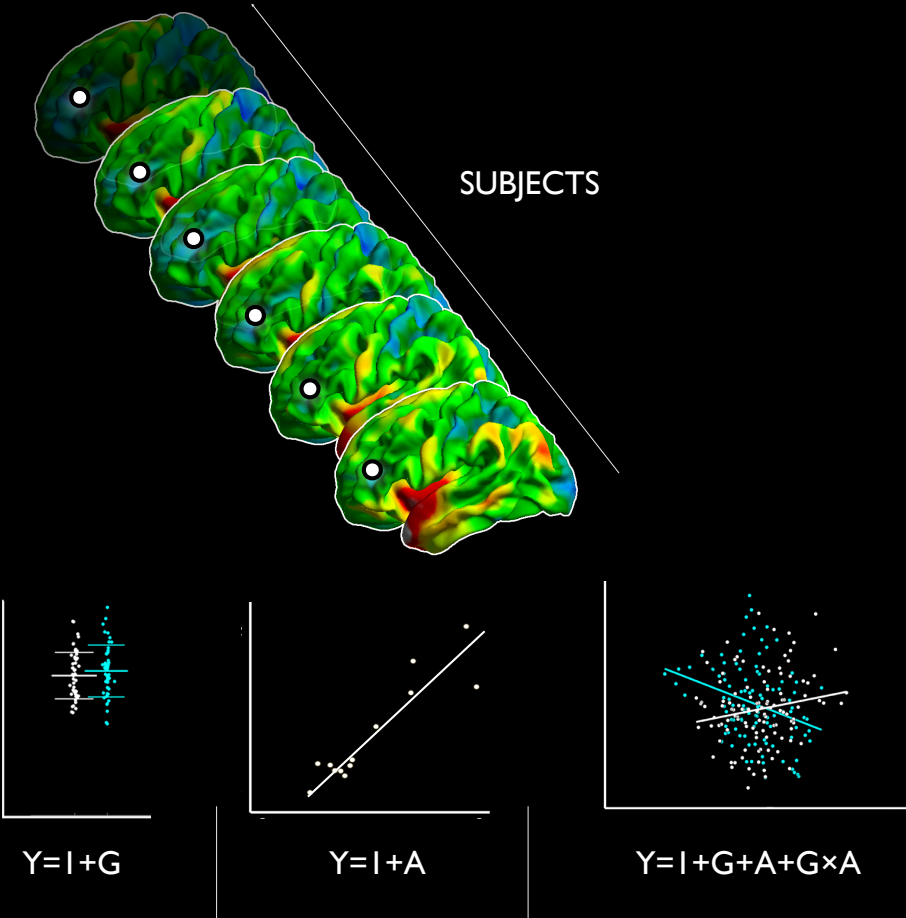


LONGITUDINAL ASSESSMENTS

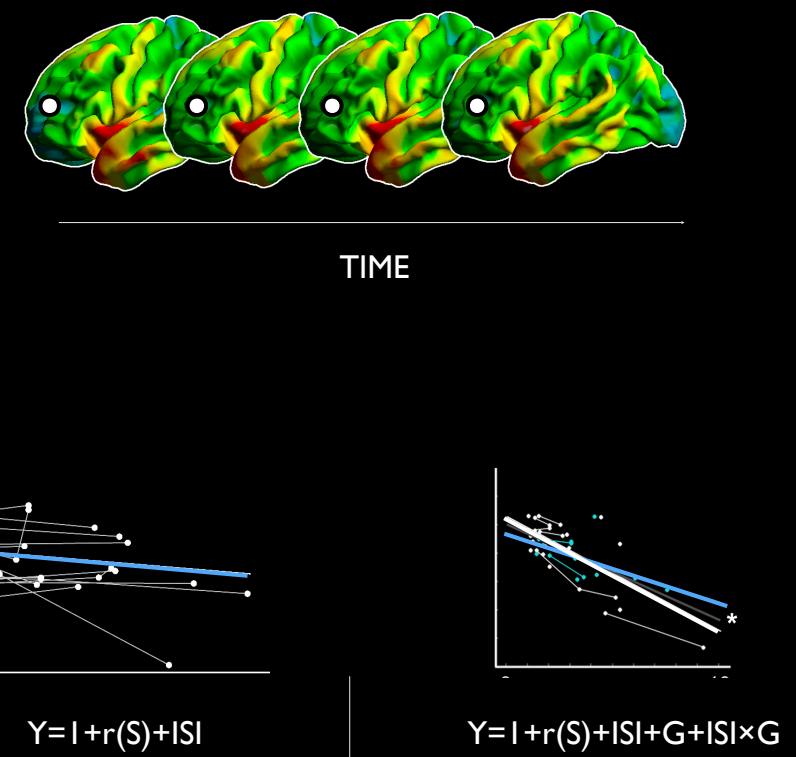


# NOW WE CAN FINALLY BUILD THE FIRST LINEAR MODELS

CROSS-SECTIONAL ANALYSES

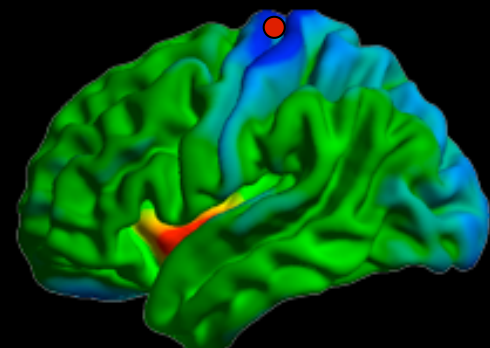


LONGITUDINAL ASSESSMENTS

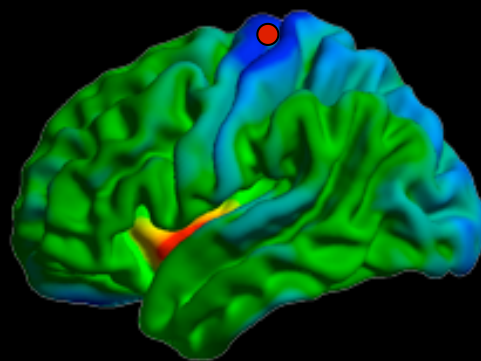


# SURFSTAT

Controls

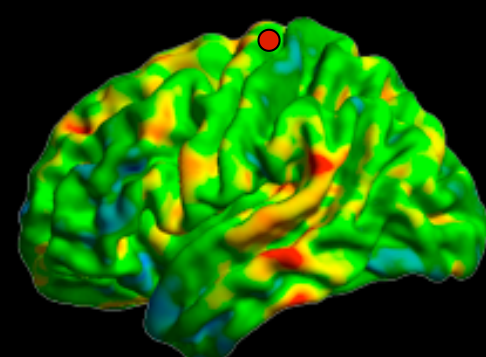


Patients

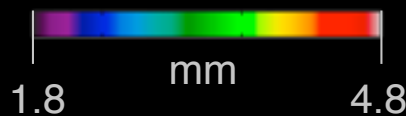
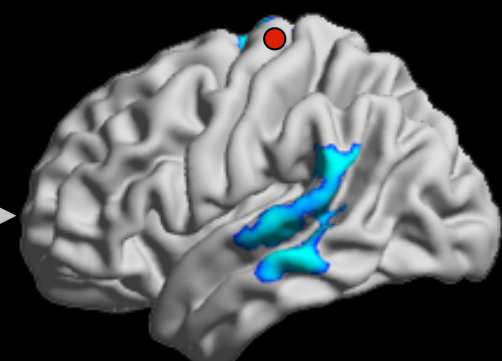


→ GLM →

t-map



p-values



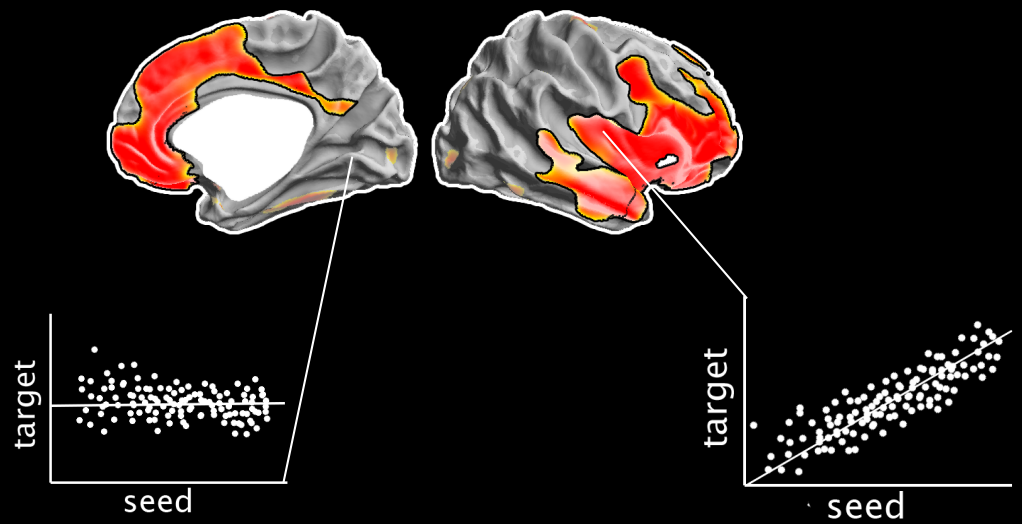
# MRI COVARIANCE ANALYSIS

A SPECIAL CASE OF A GENERALIZED LINEAR MODEL APPLICATION

THE IDEA:  
VARIABLES OF INTEREST ARE MORPHOLOGICAL MEASURES

SINGLE SEED CORRELATIONS POSSIBLE  
MODEL =  $1 + \text{SEED}$

GROUP COMPARISONS VIA INTERACTIONS  
MODEL =  $1 + \text{SEED} + \text{GROUP} + \text{GROUP}^*\text{SEED}$



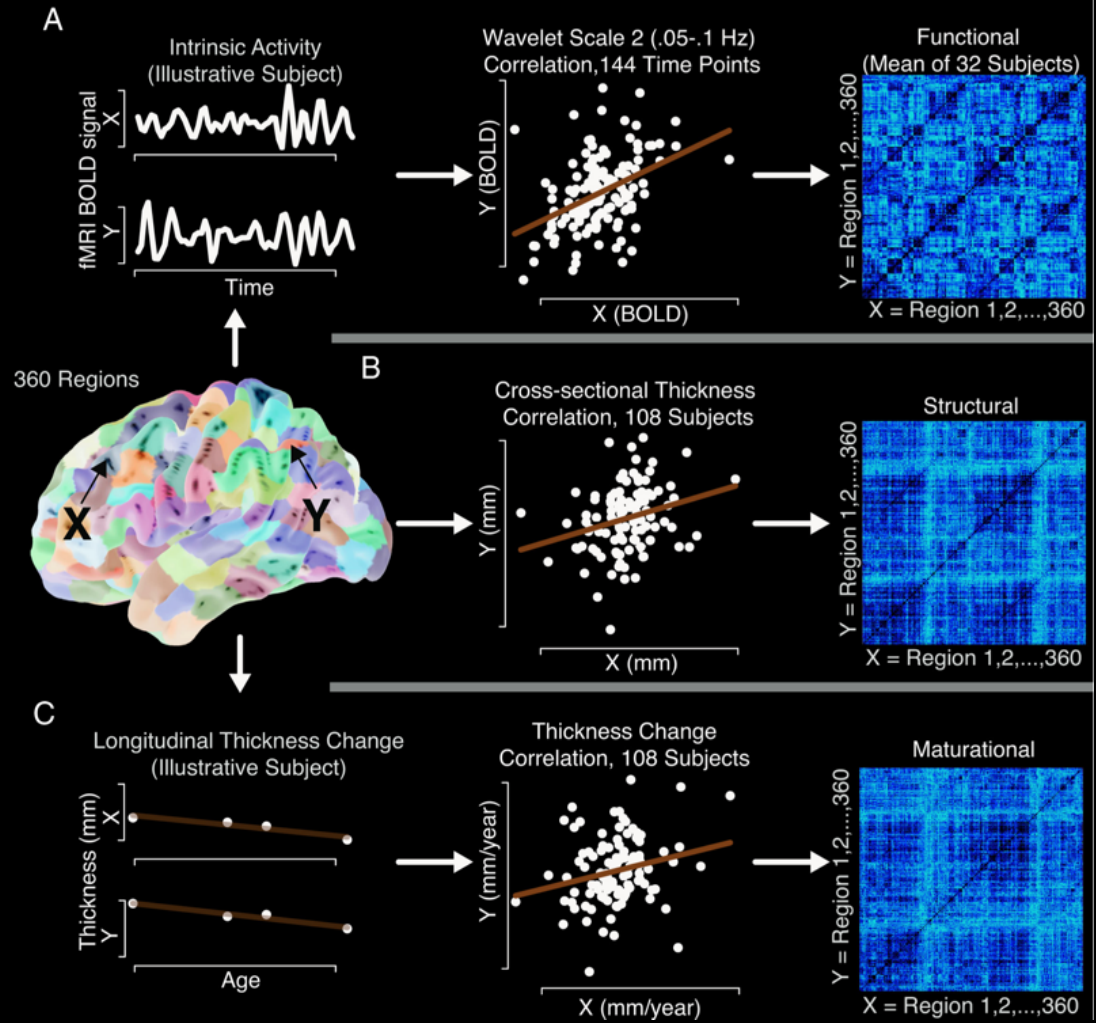
# MRI COVARIANCE ANALYSIS

AN EXTENSION OF THE COVARIANCE FRAMEWORK MAY BE A 'MATURATIONAL COUPLING ANALYSIS'

IDEA:  
INSTEAD OF USING CROSS-SECTIONAL MORPHOLOGICAL MEASURES,  
LONGITUDINAL TRAJECTORIES ARE CORRELATED

BOTH APPROACHES GIVE SIMILAR FINDINGS.  
CROSS-SECTIONAL COVARIANCE MAYBE MORE GENERAL, BUT DEPENDS ON AGE

LONGITUDINAL MATURATION ALSO DEPENDS ON AGE AND AGE-WINDOW, BUT MAY MORE SPECIFICALLY PROBE A CERTAIN PROCESS



RAZNAHAN

**Table 1. Participant Characteristics**

Characteristic	Group			Sex Difference
	All	Male	Female	
Number of Individuals	108	67	41	n.s.
Singleton	63	35	28	
Member of twin pair	45	32	13	
Handedness, No.				n.s.
Right	99	62	37	
Mixed	4	3	1	
Left	5	2	3	
Race, No.				n.s.
Caucasian	98	62	36	
African-American	3	1	2	
Asian	2	1	1	
Hispanic	3	2	1	
Other	2	1	1	
IQ				n.s.
Mean (SD)	115 (11.8)	116 (11.5)	114 (12.4)	
SES				n.s.
Mean (SD)	40 (17.6)	39 (18.5)	41 (16.2)	
Number of scans, No.				n.s.
3 scans	67	39	28	
4 scans	31	22	9	
5 scans	9	5	4	
6 scans	1	1	0	
Total	376	236	140	
Age Distribution of Scans (years)				
Mean (SD)	15.2 (3.5)	15.3 (3.5)	14.9 (3.5)	
Range	9.1–22.8	9.2–22.7	9.1–22.8	
n.s., not statistically significant at $p < 0.05$ ; SES, socioeconomic status.				

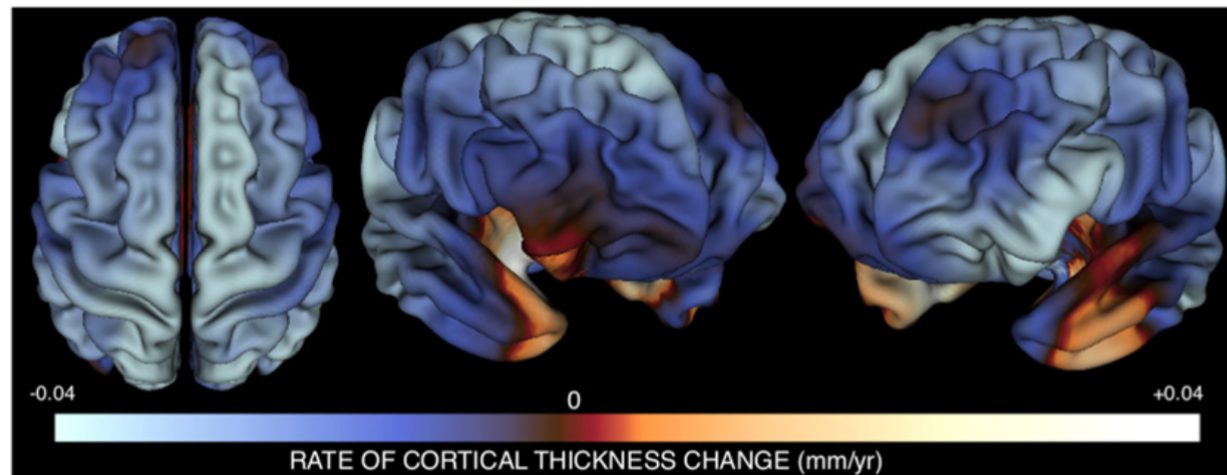
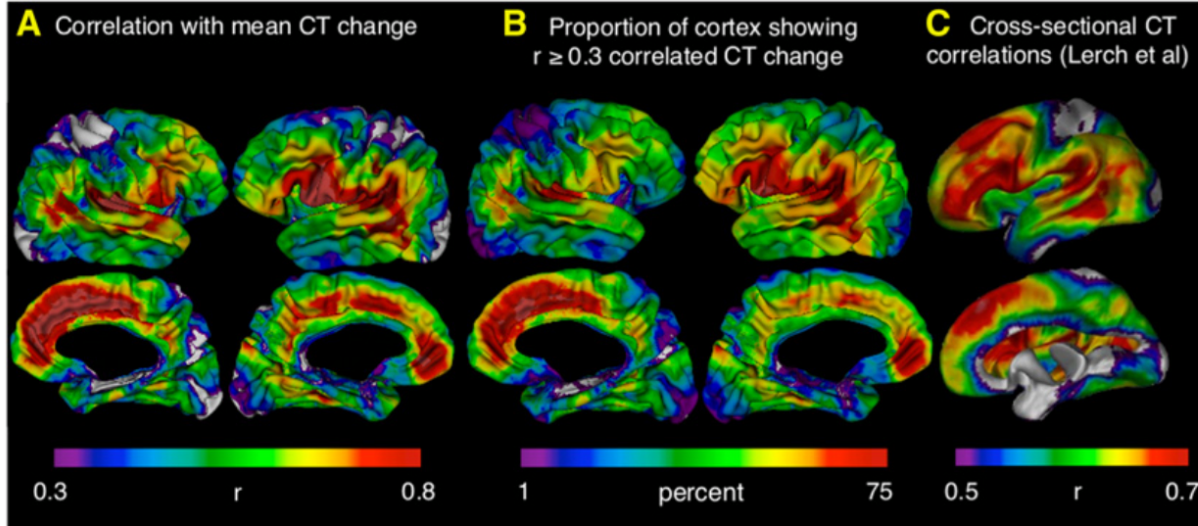


**Figure 1. Mapping the Mean Rate of CT Change per Year between Ages 9 and 22 Years using Person-Specific Estimates of CT Change**

Three views of the cortical sheet are shown. Colors represent the magnitude of mean annual cortical thickness (CT) change within our sample at each vertex. Mean change values were derived by averaging estimates of weighted annual CT change across all participants. Over the age range studied, most cortical regions are becoming thinner with advancing age, with the exception of bilateral anterior-medial temporal and right orbitofrontal cortices where CT is still increasing with age. This approach to mapping annual CT change closely replicates results derived using traditional mixed-model

approaches for analyzing longitudinal data (Figure S1), and converges with other larger mixed-model studies of CT change (Shaw et al., 2008), but has the added advantage of permitting correlational analysis of interindividual differences in CT change at different vertices.



correlated CT change with the region in question at  $r \geq 0.3$ . “Warmer” colors refer to higher proportions. Fronto-temporal regions show the most spatially extensive maturational coupling whereas primary sensory cortices show the least.

(C) A reproduction of earlier published (Lerch et al., 2006) maps showing the correlation between cross-sectional variation in CT at each vertex and mean CT across the whole vertex. Note the convergence between these maps and those for correlated CT change shown in (A) and (B).

## Figure 2. Regional Differences in Correlation with Rates of CT Change throughout the Cortical Sheet

(A) Map of correlation strength between CT change at each vertex and mean CT change across all vertices. This map has been arbitrarily thresholded at  $r \geq 0.3$  to highlight its similarity with a previously published thresholded map of cross-sectional CT correlations throughout the cortical sheet (Lerch et al., 2006). An unthresholded version of this map is provided in Figure S2A. Note that the strongest correlations with mean CT change are seen in fronto-temporal association cortices, whereas weakest correlations with mean CT change are seen in primary sensory cortices.

(B) An alternative representation of regional differences in maturational coupling. The color at a given cortical region represents the proportion of the cortical surface showing

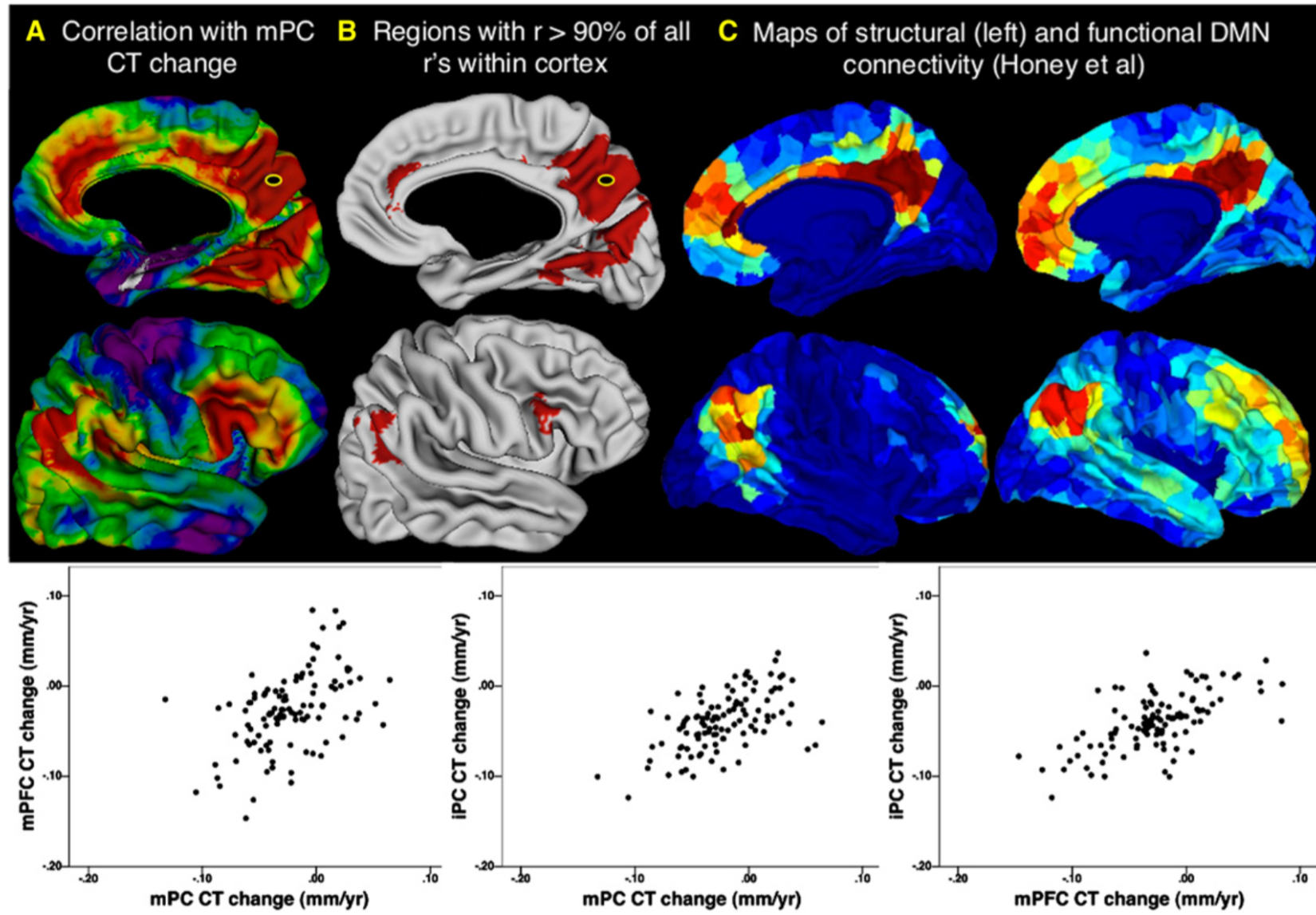


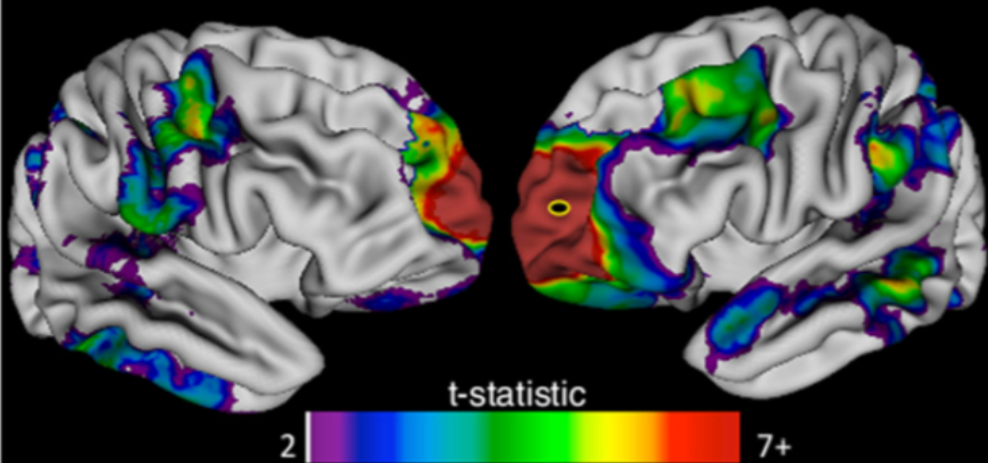
**Figure 3. Maturational Coupling within the Default Mode Network**

(A) Right hemisphere map of maturational coupling with the medial posterior cortex (mPC) default mode network (DMN) node. Color gradations represent correlation centile position in the distribution of all possible correlations between cortical vertices (blue → red: 1st → 100th centile).

(B) Regions where correlations with mPC change are in the top 90% of all possible correlations. Note mPFG and iPC overlaps between the distribution of regions showing highly coordinated maturation with the mPC DMN seed, and the distribution of regions that show high functional and structural connectivity within the DMN.

(C and D) Figures from Honey et al. (2009) depicting the DMN by analysis of diffusion tensor imaging and functional magnetic resonance data, respectively.

**A** Regions showing significant coupling with left frontopolar maturation in both sexes



**B** Regions showing significant sexually-dimorphic coupling with left frontopolar maturation

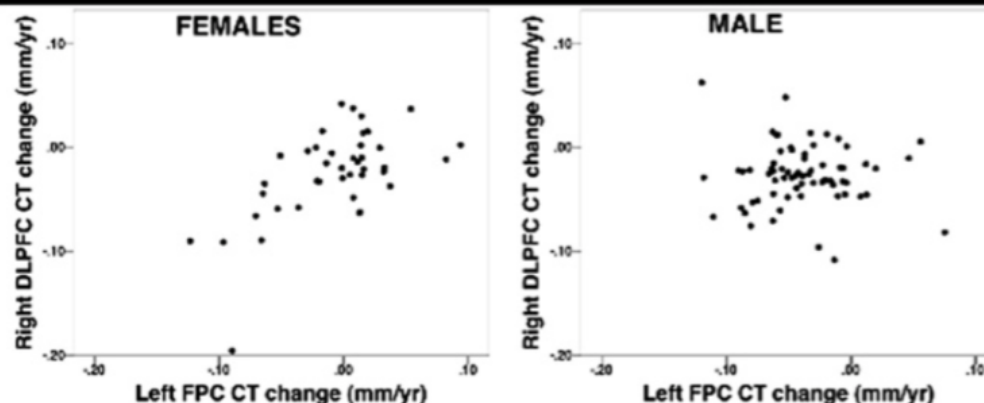
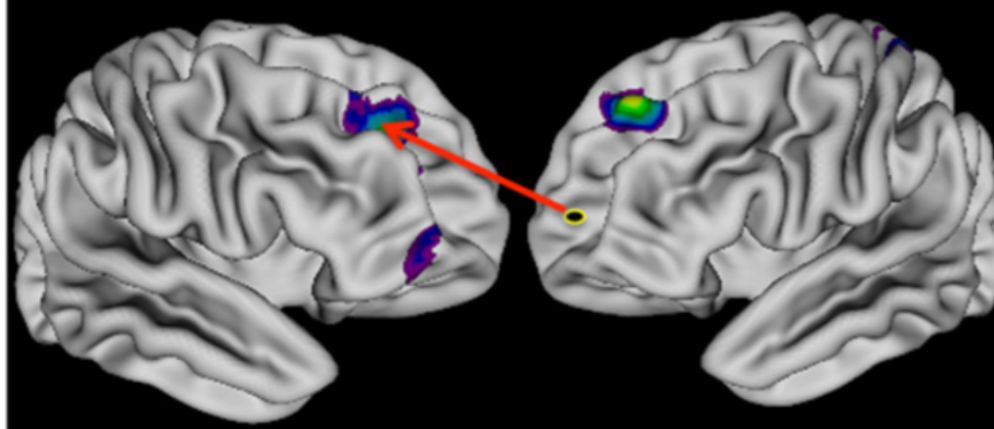


**Figure 4. Maturational Coupling with the Left Frontopolar Cortex and Its Variation by Sex**

The left frontopolar cortex (FPC) was used as a seed to explore sex differences in maturational coupling because it is where rate of cortical thickness (CT) change shows statistically significant sex differences over the age range studied—in both prior work (Raznahan et al., 2010; Figure S4A) and our current study (Figure S4B).

(A) Map of regions showing significant maturational coupling with left FPC that is not significantly different in magnitude between males and females. Note the very strong relationship between left FPC change and change at its contralateral homolog. Several regions show bilateral coupling with IFPC change (e.g., inferior temporal, planum temporale, angular gyrus and orbitofrontal cortex).

(B) Regions where coupling with IFPC CT change differs significantly between males and females. These consist of areas where coupling is specific to females, as shown for the right dorsolateral prefrontal cortex (rDLPFC) in the inset scatter plot. Furthermore, sex differences in FPC-DLPFC coupling also remained statistically significant after removal of nine outliers (defined using a conservative Cooks distance threshold of  $4/n$ ).

LEBEL & BEAULIEU

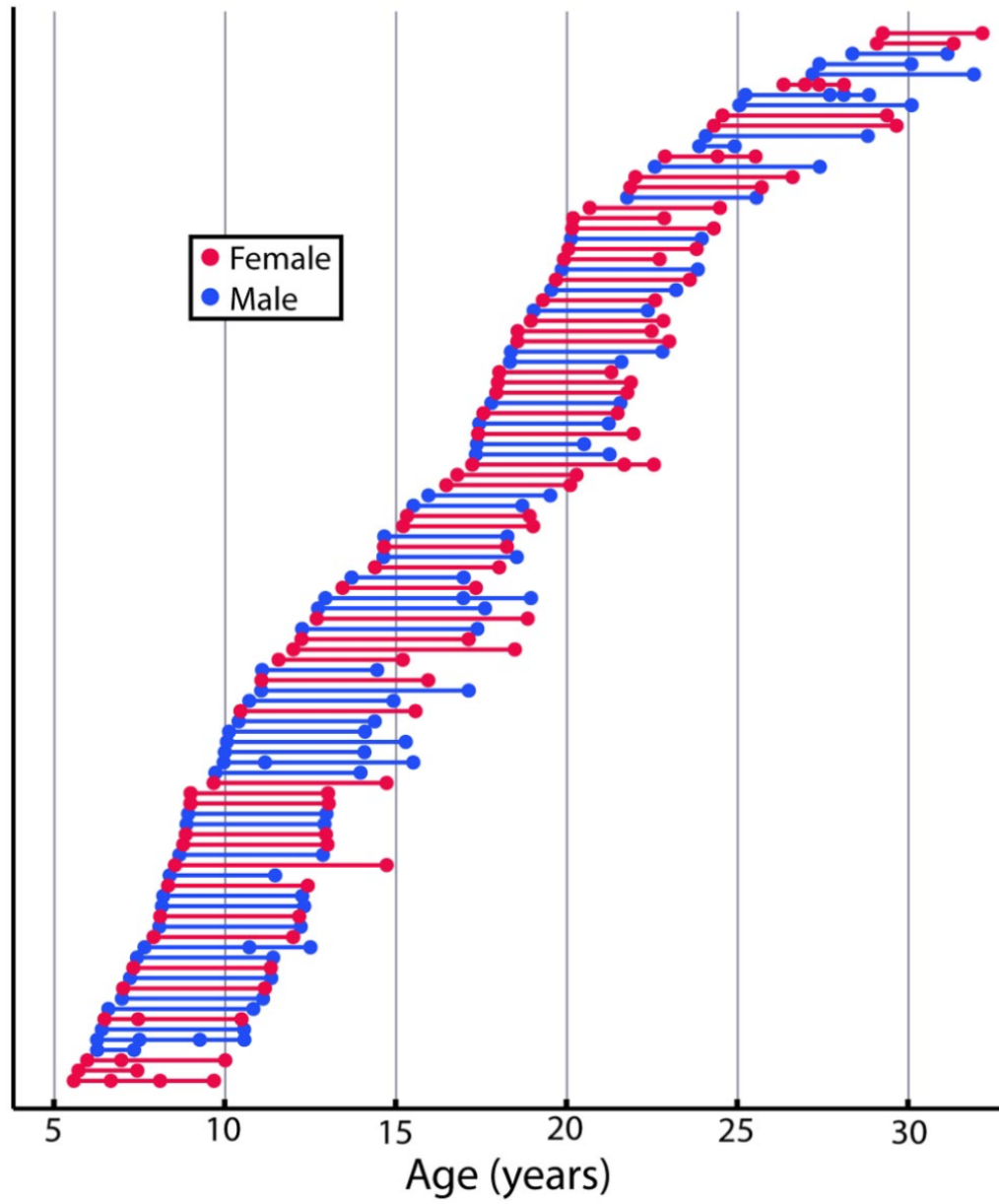
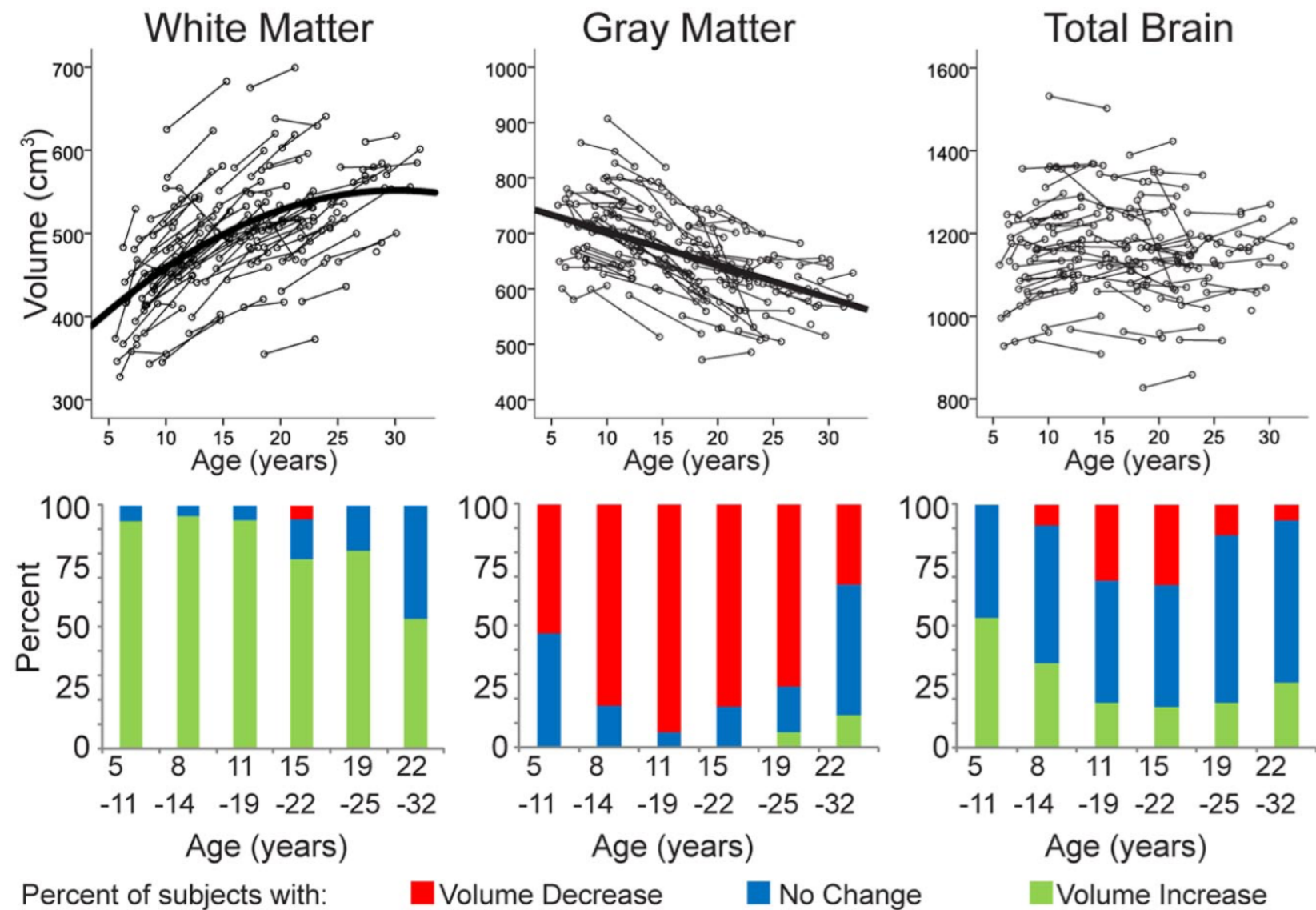


**Figure 1.** Age at scans for all subjects. Each of the 221 scans obtained is represented by a circle; each of the 103 subjects is shown in a different row, with their scans connected by a straight line. Females (red) and males (blue) are marked separately. Note the relatively even spacing of subjects across the age range, with most subjects receiving two scans  $\sim$ 4 years apart. Several subjects received three or four scans in total.

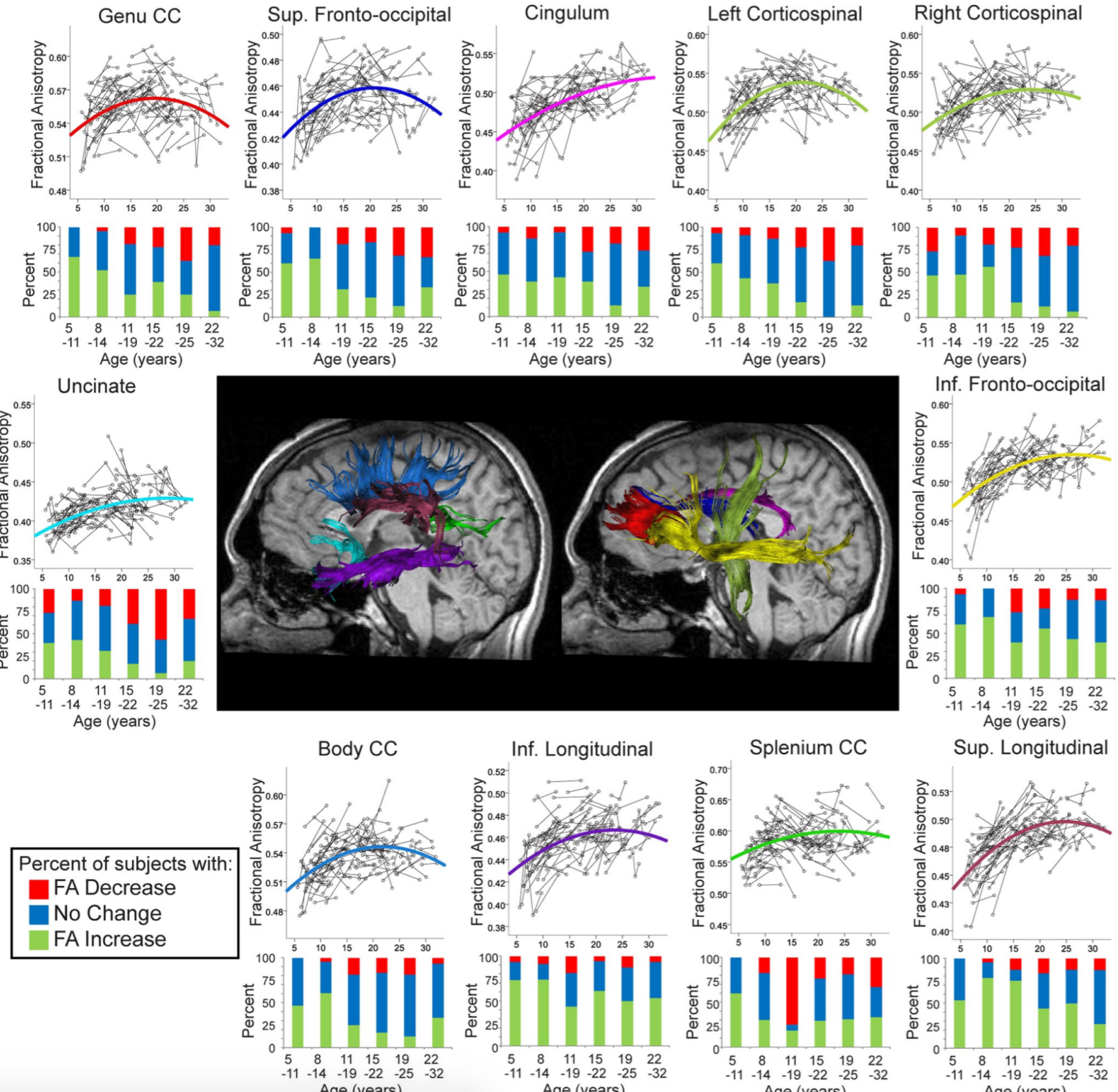
**Table 1. Tractography-derived SDs over multiple scans**

Tract	FA	MD ( $\times 10^{-3}$ mm $^2$ /s)	$\lambda_{//}$ ( $\times 10^{-3}$ mm $^2$ /s)	$\lambda_{\perp}$ ( $\times 10^{-3}$ mm $^2$ /s)	Volume (cm $^3$ )
Genu of the corpus callosum	0.012	0.017	0.023	0.016	1.15
Body of the corpus callosum	0.013	0.022	0.034	0.020	2.29
Splenium of the corpus callosum	0.012	0.024	0.032	0.022	1.06
Corticospinal tract	0.019	0.025	0.030	0.025	1.23
Cingulum	0.016	0.012	0.020	0.017	0.54
Inferior longitudinal fasciculus	0.007	0.012	0.017	0.012	1.27
Inferior fronto-occipital fasciculus	0.012	0.012	0.022	0.011	2.65
Superior longitudinal fasciculus	0.009	0.010	0.012	0.012	1.25
Superior fronto-occipital fasciculus	0.009	0.011	0.013	0.012	0.72
Uncinate fasciculus	0.010	0.012	0.025	0.022	0.83

Seven subjects were scanned three to four times each within 6 months to determine reliability of the diffusion and tract volume measurements over time. The mean of the SDs over all scans per subject are shown for each parameter [FA, MD, parallel ( $\lambda_{//}$ ) and perpendicular diffusivity ( $\lambda_{\perp}$ ), and tract volume], which were then used as a threshold for determining whether the parameters increased or decreased between scans in the study population.



**Figure 2.** Longitudinal volume changes on T1-weighted images. Changes of white matter, gray matter, and total brain volume with age for each scan are shown (top row) along with bar graphs reflecting the percentage of subjects with volume increases (green), decreases (red), or no change (blue) within six age categories. White matter volume increased significantly across the age range, including the twenties, while gray matter volume decreased in the majority of children, adolescents, and young adults up to 25 years. These white matter increases and gray matter decreases offset one another such that total brain volume did not change in most persons, although many of the younger subjects had small increases.



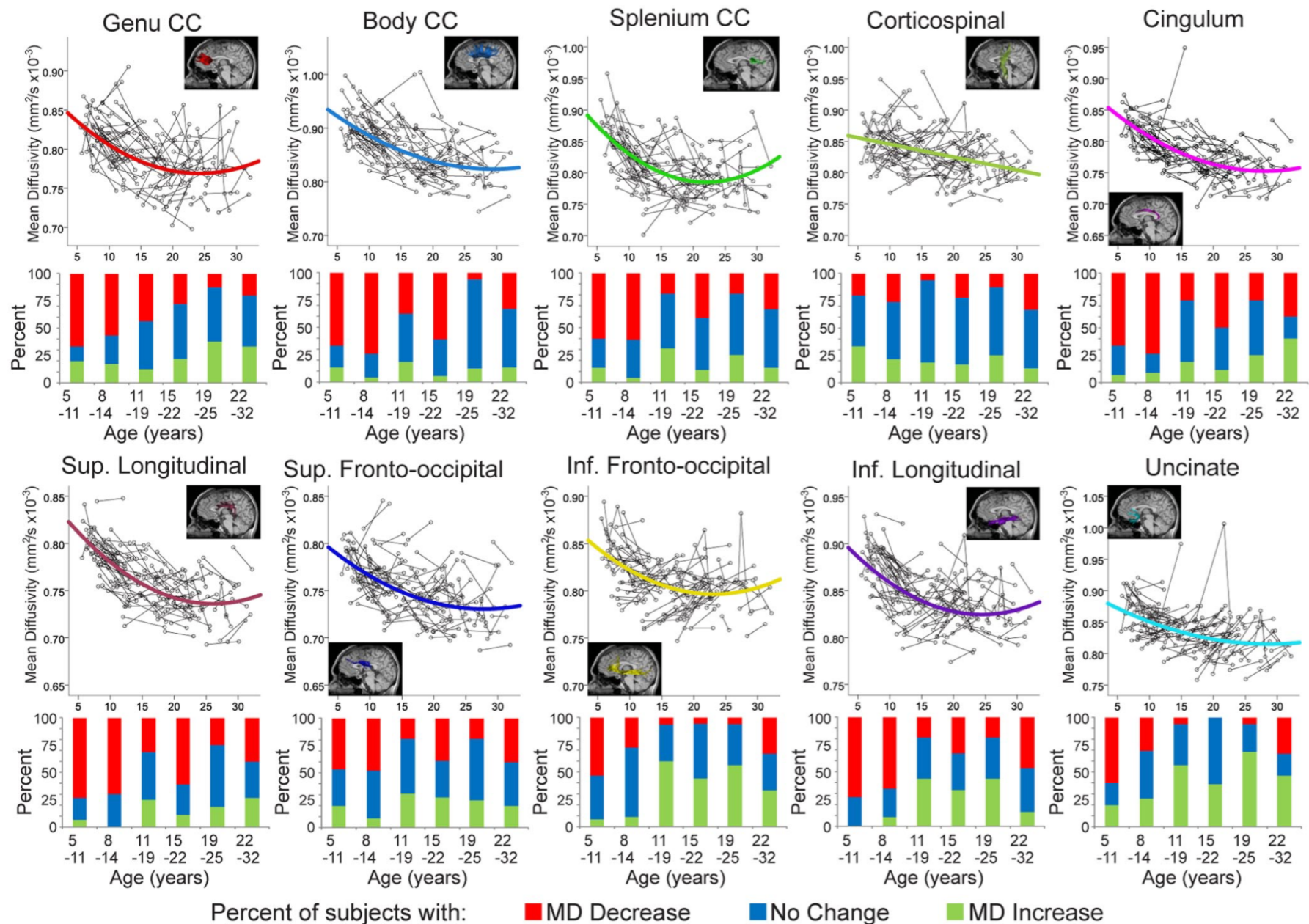


**Figure 4.** Longitudinal age-related changes of mean diffusivity. All 10 tracts had significant age-related decreases of MD. Commissural tracts demonstrated expected patterns, where a large proportion of subjects had decreasing MD in childhood and there were fewer subjects with decreases at older ages. Most association tracts, however, demonstrated more prolonged MD decreases, with 30–40% of older subjects having decreases of MD between scans. Notably, the inferior fronto-occipital, inferior longitudinal, and uncinate fasciculi show 40–60% of subjects with increasing MD between scans as early as the 11–19 year group. Other frontal lobe connecting white matter fibers, such as the genu of the corpus callosum and the cingulum, demonstrate 30–40% of subjects with increasing MD but only in the oldest age grouping of 22–32 years suggesting age-related decline is beginning in some subjects.

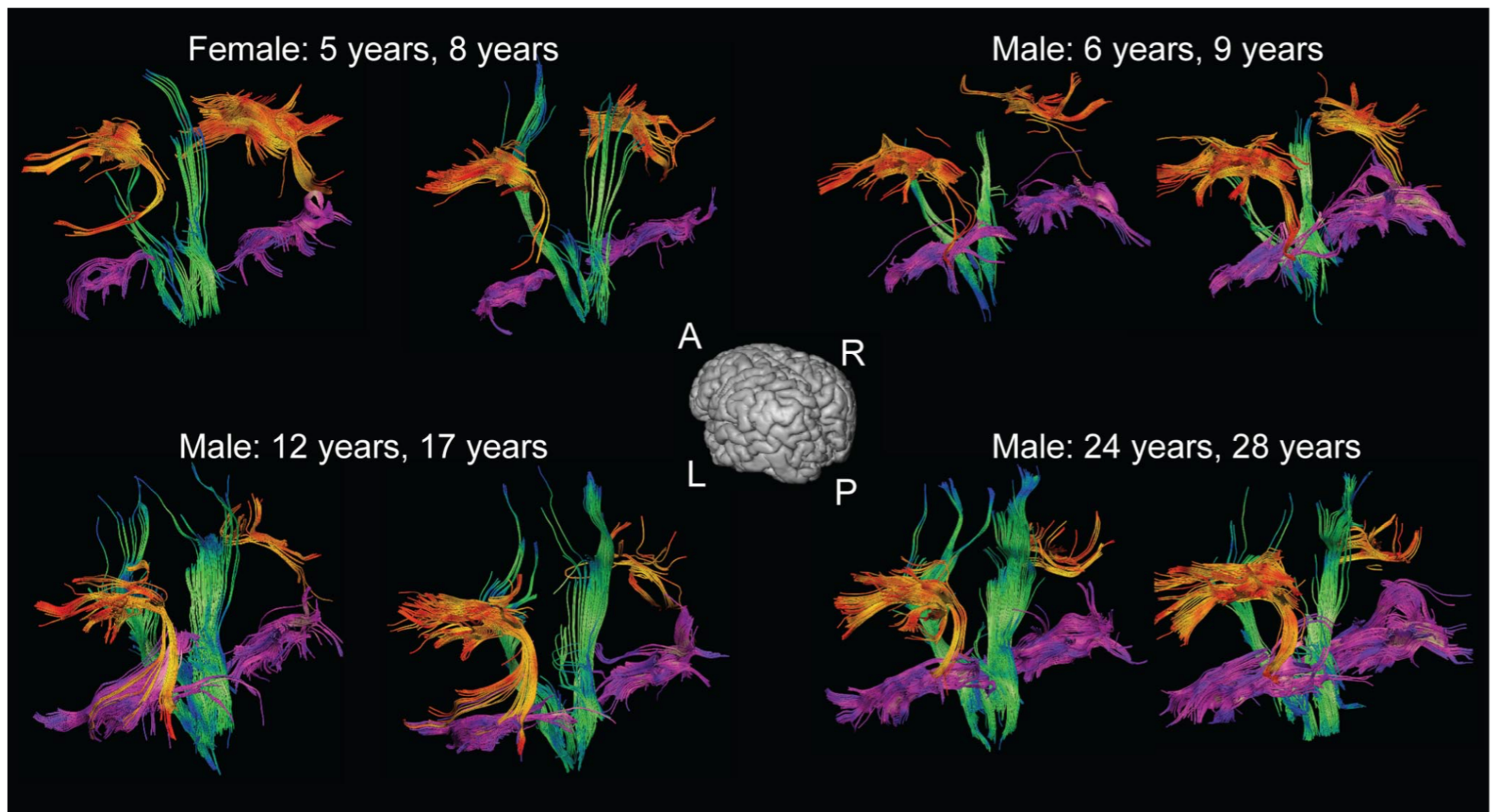


**Figure 5.** Sample tracts at two time points. Tracts are shown at two time points for several individuals. The superior longitudinal fasciculus (orange), corticospinal tract (green), and inferior longitudinal fasciculus (purple) are given as examples because they can be some of the more difficult and inconsistent fibers to track. Note that, although there are considerable variations in length, size, and shape of the tracts among individuals, the tracts look relatively similar within the same individual.

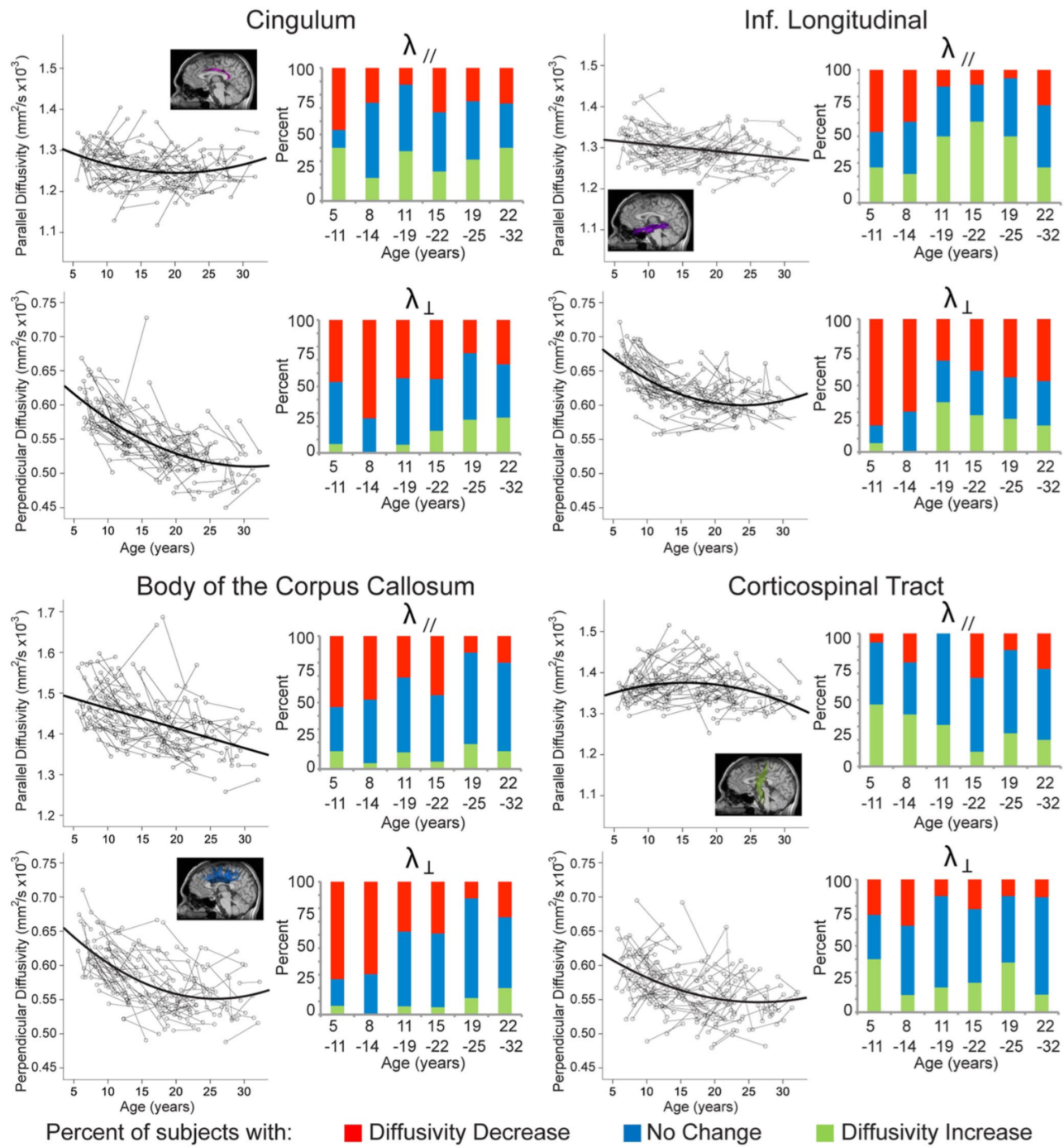


**Figure 6.** Longitudinal changes of parallel and perpendicular diffusivity. For all tracts, most young subjects had decreased perpendicular diffusivity between scans and fewer older subjects had decreases. Parallel diffusivity trajectories varied more among tracts. Most association fibers (such as the cingulum shown above) had only small changes of parallel diffusivity, although for tracts with prolonged FA changes (superior and inferior longitudinal, shown above, and inferior fronto-occipital fasciculi), a substantial portion of older subjects demonstrated increased parallel diffusivity between scans. Commissural fibers had substantial decreases of both parallel and perpendicular diffusivity in young subjects, with most subjects having no change at older ages. The corticospinal tract was unique in that its parallel diffusivity trajectory increased at young ages; its perpendicular diffusivity trajectory was similar to that of other tracts.

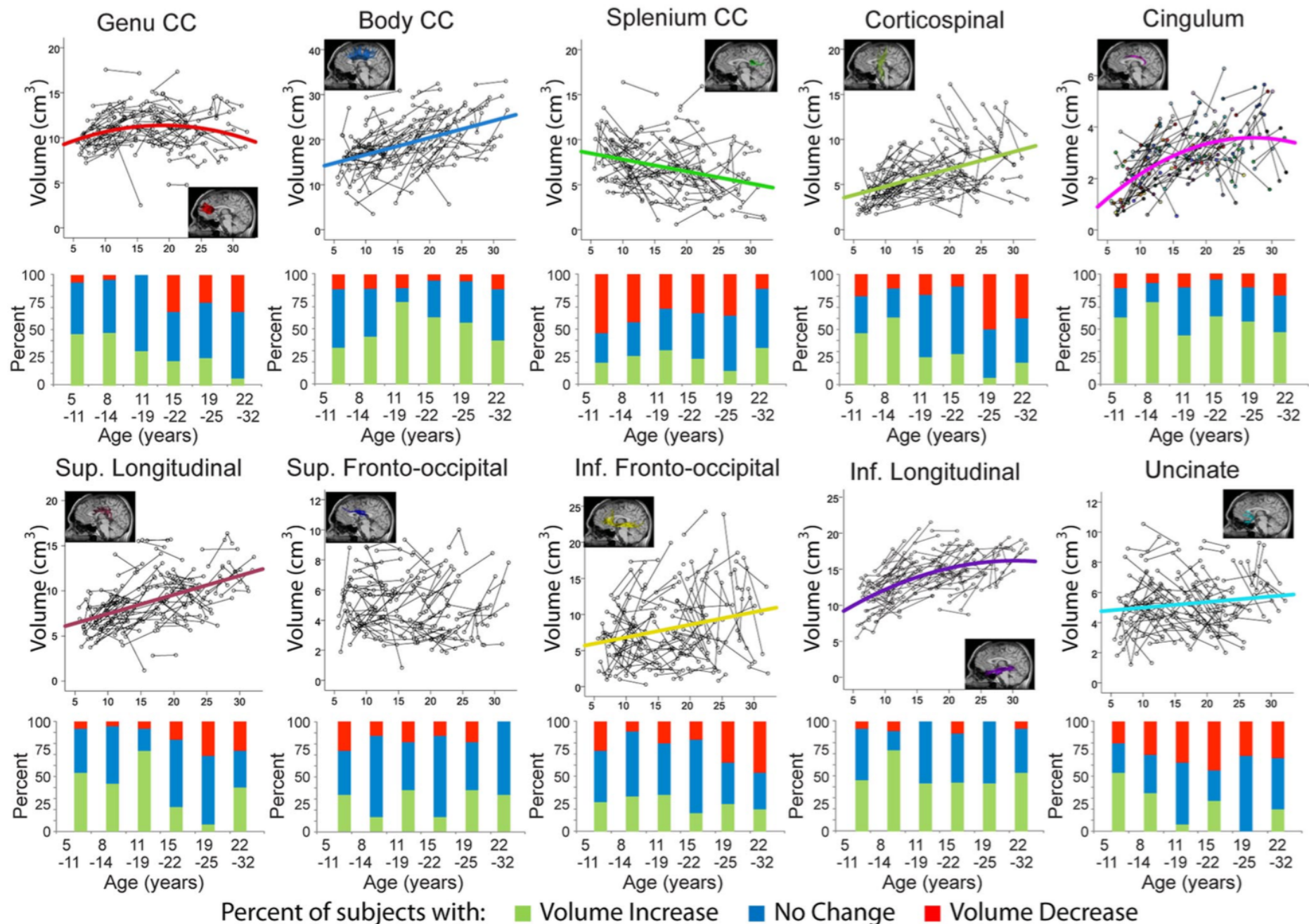


**Figure 7.** Longitudinal changes of tract volume. Volume changes were significant for most tracts, although not for the superior fronto-occipital fasciculus (no trend line shown). Most tracts had linear volume increases across the age range, although the cingulum, genu of the corpus callosum, and the inferior longitudinal fasciculus had quadratic trends with increases then decreases, and the splenium of the corpus callosum showed linear decreases of volume. Note that within-subject increases of tract volumes were observed in 40–50% of subjects in the 19–25 and 22–32 year age groups for the body of the corpus callosum, cingulum, and inferior longitudinal fasciculus.

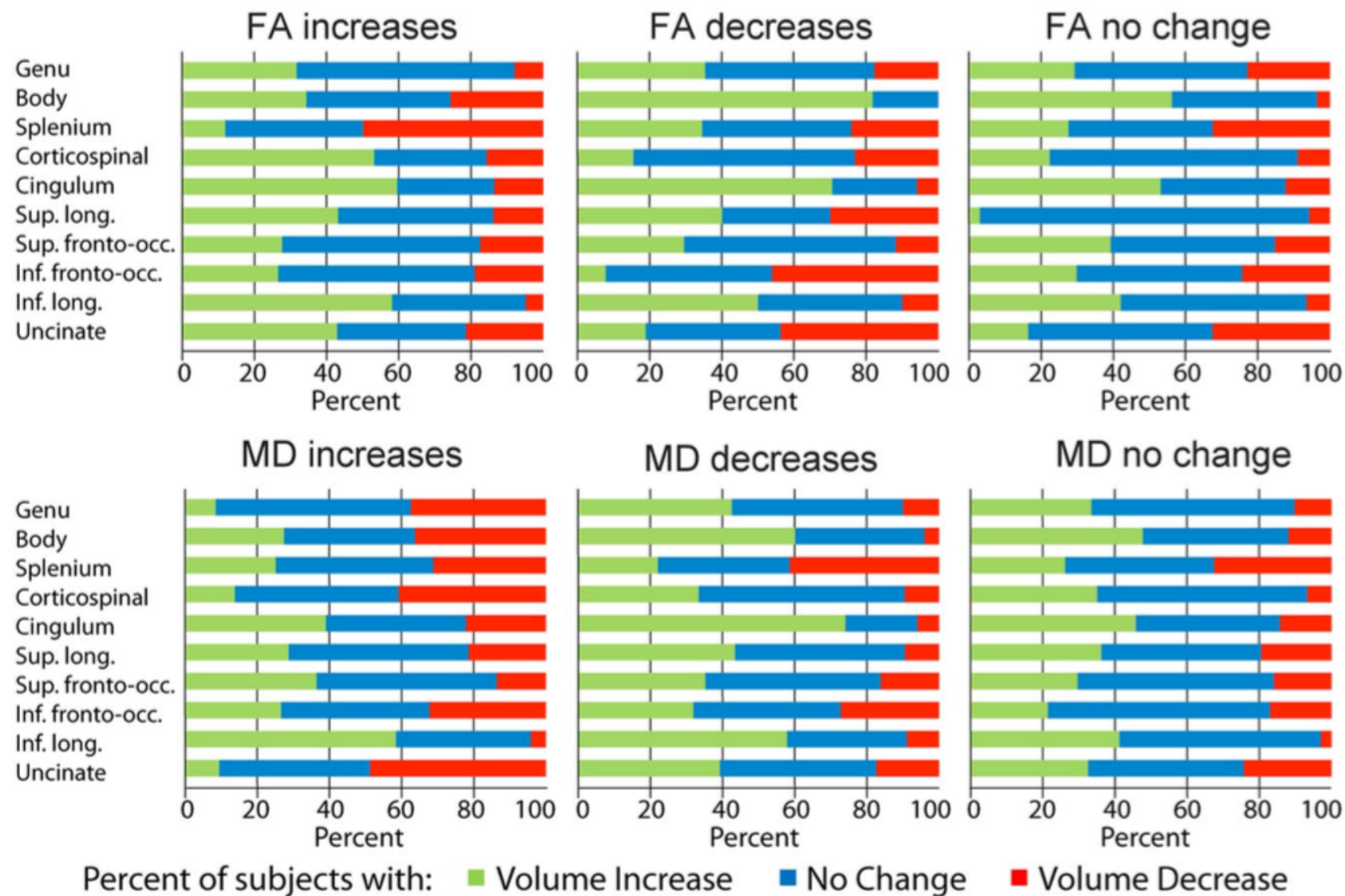


**Figure 8.** Tract volume relationship with FA and MD changes. The percentage of subjects that showed increases (green), decreases (red), or no change (blue) in tract volume between scans are shown for each group depending on the evolution of FA or MD. While there is a decent proportion of subjects with elevated FA or reduced MD that have increased tract volume, there is a greater proportion of subjects with no change or even a decrease in tract volume in these cases. There is no clear association between tract volume and diffusion parameter changes.